

# Hydrolysis Precipitation-assisted Solid-state Reaction to $\text{Li}_4\text{Ti}_5\text{O}_{12}$ and its Electrochemical Properties

Jie Xu, Chunju Lv\* and Guanglei Tian

College of Materials and Engineering, China Jiliang University, Hangzhou, PR China

Received: June 28, 2011, Accepted: September 13, 2011, Available online: October 13, 2011

**Abstract:** Spinel lithium titanate ( $\text{Li}_4\text{Ti}_5\text{O}_{12}$ ) materials were synthesized by a hydrolysis precipitation-assisted solid-state method in the temperature range from 600 to 900 °C for large-scale production. DSC/TGA, XRD and SEM were used to characterize the as-prepared samples. The optimum synthesis condition was examined in relation to the charge–discharge performance. It was found that when the dry hydrolysis precipitation precursor with 8% Li excess was calcined at 700–800 °C for 12 h in air, a pure  $\text{Li}_4\text{Ti}_5\text{O}_{12}$  phase was obtained. The as-obtained material has the best electrochemical performance due to its narrow size distribution and precise stoichiometry of the oxide.

**Keywords:** lithium-ion battery; electrochemical performance;  $\text{Li}_4\text{Ti}_5\text{O}_{12}$

## 1. INTRODUCTION

In recent years, spinel  $\text{Li}_4\text{Ti}_5\text{O}_{12}$  is being considered as one promising alternative to graphite to be an anode material for lithium-ion batteries.  $\text{Li}_4\text{Ti}_5\text{O}_{12}$  has an excellent cycle performance due to its small volume change (the so-called zero-strain material) during charge–discharge cycling [1], excellent lithium insertion–extraction reversibility and a high theoretical capacity of 175  $\text{mAh}\cdot\text{g}^{-1}$ . It has very flat charge and discharge curves and the potential for Li-insertion is about 1.55 V vs.  $\text{Li}^+/\text{Li}$  [1-3], which is above the potential range where most electrolytes are reduced. This makes  $\text{Li}_4\text{Ti}_5\text{O}_{12}$  a promising anode material of lithium ion batteries for safety concerns [4]. Although its medium level of discharge voltage discourages the application as a positive electrode,  $\text{Li}_4\text{Ti}_5\text{O}_{12}$  can be coupled with a high-voltage electrode such as  $\text{LiMn}_2\text{O}_4$ ,  $\text{LiCoO}_2$ ,  $\text{LiCoPO}_4$  or  $\text{LiFePO}_4$  to provide a cell with an operating voltage above 2.0 V [4-8].

The synthesis process plays a major role in improving the physicochemical properties of the electrode materials. And it is well known that the use of nanophase  $\text{Li}_4\text{Ti}_5\text{O}_{12}$  as electrode reduces the diffusion length leading to improved lithium intercalation kinetics [9-11]. Moreover, the use of nanomaterials allows for an increased number of active sites for surface reaction decreasing the local current density which, in turn, lowers the over potential and leads

to high rate capability [12, 13]. Various techniques for the preparation of nanostructured  $\text{Li}_4\text{Ti}_5\text{O}_{12}$  have been reported in the literatures. These include emulsion gel [14], spray drying [15], hydrothermal [16-18], and sol–gel method [19-25]. However, such wet chemical synthesis methods are complicated and always require a non-aqueous medium which increases the cost. Up to now, the solid-state reaction is still the most attractive process for potential industrial application because it has a series of advantages such as simple process, without using solvent and friendly to the environment. In most of previous works, using bulk  $\text{TiO}_2$  and  $\text{Li}_2\text{CO}_3/\text{LiOH}/\text{LiAc}$  as the raw materials, high-temperature calcination and prolonged time were always necessary to improve the phase purity [26-31]. These synthetic conditions (for example, sintering time and temperature), which require long-range diffusion of the reactants, may result in non-homogeneity, irregular morphology, large particle size, broad particle size distribution, and poor control of stoichiometry. In order to avoid the problem above mentioned, the precision control of starting mixture is very important to decrease the temperature and time of calcination and prepare  $\text{Li}_4\text{Ti}_5\text{O}_{12}$  in nanometer regime.

In this study, we obtained the starting mixture precursor by hydrolysis precipitation using the raw materials of tetrabutyl titanate ( $\text{Ti}(\text{OC}_4\text{H}_9)_4$ ), lithium acetate ( $\text{LiAc}\cdot 2\text{H}_2\text{O}$ ). The conditions to prepare spinel  $\text{Li}_4\text{Ti}_5\text{O}_{12}$  with narrow size distribution were optimized, and the electrochemical properties of the prepared  $\text{Li}_4\text{Ti}_5\text{O}_{12}$  were characterized.

\*To whom correspondence should be addressed: Email: lvchunju@cjl.u.edu.cn

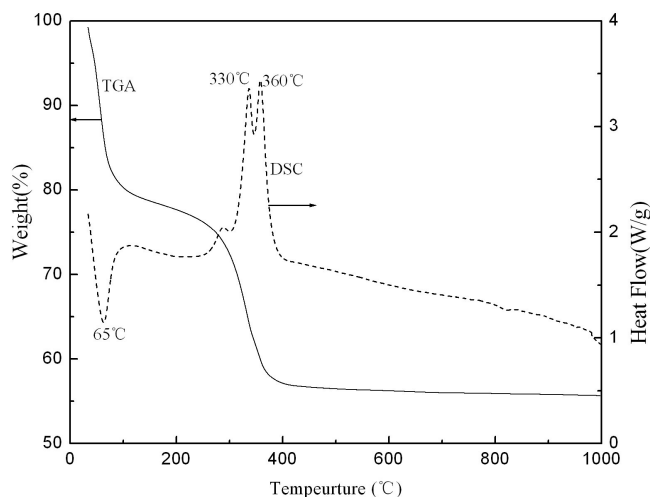


Figure 1. TGA and DSC curves of the dry precursor powders prepared from hydrolysis precipitation with 8% Li excess.

## 2. EXPERIMENTAL

### 2.1. Sample preparation and characterization

All chemicals were used as received. Tetrabutyl titanate (CP) was procured from Shanghai Meixing Industries Co. Ltd., China and lithium acetate (AR) from Shanghai Hengxin Chemical Reagent Co. Ltd., China. Typically, 0.5 mol of tetrabutyl titanate was dissolved in ethanol to obtain solution A. A stoichiometric lithium acetate with a Li:Ti molar ratio of 4:5 was dissolved in deionized water to obtain solution B. To compensate for the  $\text{Li}_2\text{O}$  sublimation during the thermal treatment, a  $\text{LiAc}\cdot 2\text{H}_2\text{O}$  weight excess from 2% to 10% was adopted. Then, the  $\text{LiAc}$  aqueous solution was dropped slowly into  $\text{Ti}(\text{OC}_4\text{H}_9)_4$  ethanol solution under magnetic stirring. In this dropping process, the solution turn to white as  $\text{Ti}(\text{OC}_4\text{H}_9)_4$  hydrolyzing. After 1 h stirring, the white solution was treated at 80 °C to remove solvents gradually, and became a precursor finally. Then, the dry precursor was ground and calcined at different temperature for 12 h in air at a heating rate of 5 °C/min, followed by natural cooling in the furnace. Finally, a white powder with amount of about 45 g was obtained. All electrode active samples were prepared according to above sequence.

The thermal analysis (TGA-DSC, SDT Q600) to determine suitable temperatures for calcining the precursor were performed with  $\alpha\text{-Al}_2\text{O}_3$  as the reference substance at a heating rate of 5 °C. $\text{min}^{-1}$  in air. The crystal structures of the as-prepared powders were carried on X-ray diffractometry (XRD, RIGAKU DMAX-33) using Cu K $\alpha$  radiation ( $\lambda = 1.5418 \times 10^{-10}$  m). The morphological characteristics of the powders were investigated using scanning electron microscopy (SEM, Hitachi TM3000).

### 2.2. Electrode preparation and electrochemical characterization

A two electrode coin-type cell (CR 2032) was fabricated for charge-discharge tests. To make the working electrode, 80 wt.%  $\text{Li}_4\text{Ti}_5\text{O}_{12}$ , 10 wt.% super-P carbon, and 10 wt.% polyvinylidene fluoride (PVdF) were mixed well together in *N*-methyl pyrrolidone (NMP). The prepared slurry was spread uniformly on current col-

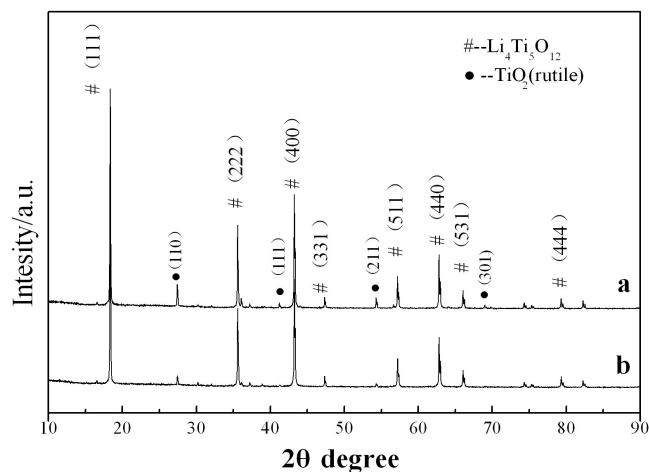


Figure 2. XRD patterns of the samples calcined at 800 °C for 12h with (a) no Li excess, (b) 8% Li excess. The main diffraction peaks of  $\text{Li}_4\text{Ti}_5\text{O}_{12}$  and rutile phase  $\text{TiO}_2$  are marked in the diagram.

lectors of copper foil (10  $\mu\text{m}$ ), and it was dried overnight at 100 °C in vacuum. The test cell is a two-electrode system and all of the cells were assembled in a glove box filled with dry argon gas. A lithium foil was used as the counter electrode, and a microporous polypropylene film (Celgard, 2400) was used as the separator. An equal volume of the ethylene carbonate (EC) and diethyl carbonate (DEC) (1:1) solvent with 1M lithium hexa-fluoro-phosphate ( $\text{LiPF}_6$ ) salt was used as an electrolyte. The polypropylene membrane was soaked in the electrolyte for 24 h prior to use. The specific capacity and current density were based on the active material ( $\text{Li}_4\text{Ti}_5\text{O}_{12}$ ) only, which was typically 6–7 mg per electrode with a surface area of about 2  $\text{cm}^2$ .

Galvanostatic charge-discharge test was performed using automatic charge-discharge equipment (Land 2001A) in a potential range of 1.0–3.0 V versus  $\text{Li}^+/\text{Li}$  electrode at 0.1 C rate (16.7  $\text{mA}\cdot\text{g}^{-1}$ ). All electrochemical experiments were conducted at room temperature with a constant humidity.

## 3. RESULTS AND DISCUSSION

DSC/TGA was performed on the dry precursor powders prepared from hydrolysis precipitation with 8% Li weight excess, which was provided to compensate for the loss of Li during thermal treatment according to the other researchers' work [32]. The thermal treatment temperature is in the range of 30 to 1000 °C. The result is shown in Fig.1. The figure clearly shows a step-like pattern of weight loss for the precursor. There are two distinct steps of weight loss. The first step of weight loss below 100 °C is attributed to the vaporization of residual organic substance and the decomposition of water from  $\text{LiAc}\cdot 2\text{H}_2\text{O}$  in the precursor powders. The weight loss is about 22% in this process. The endothermic peak in the DSC curve centered at 65 °C comes from the melt of  $\text{LiAc}$ . The weight loss of the second step is about 25%. But two strong exothermic peaks are observable in this stage. The exothermic peak centered at 330 °C is due to the decomposition of the containing  $\text{Ti}(\text{OH})_4$  in the

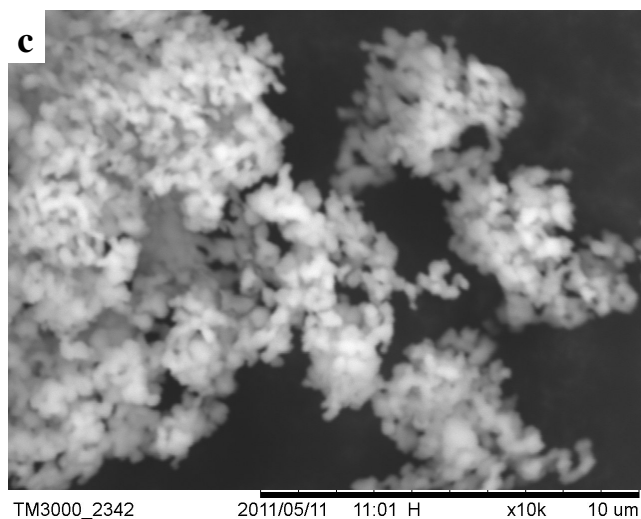
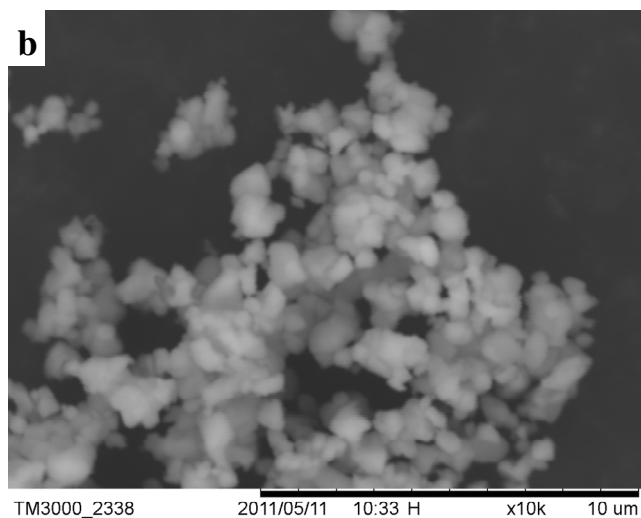
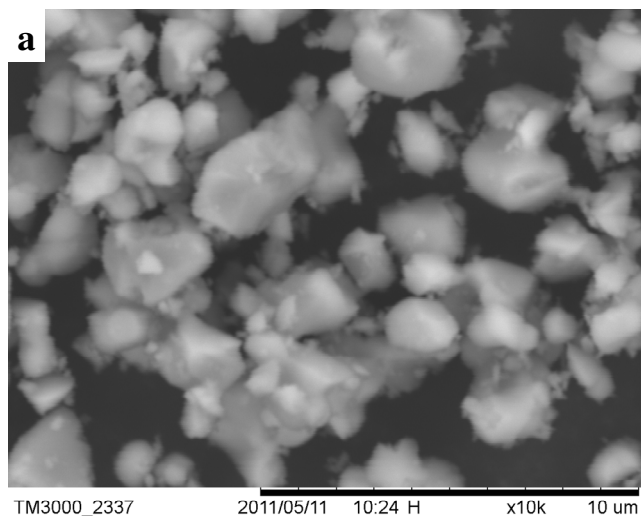


Figure 3. SEM images of the samples with (a) no Li excess, (b) 8% Li excess calcined at 800 °C for 12h and (c) 8% Li excess calcined at 750 °C for 12h.

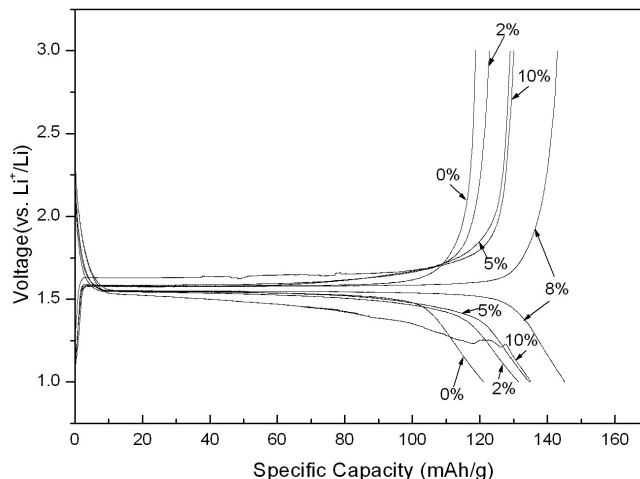


Figure 4. The initial charge-discharge profiles of the as-prepared oxides with different Li excess from 1 to 3V at 0.1C rate.

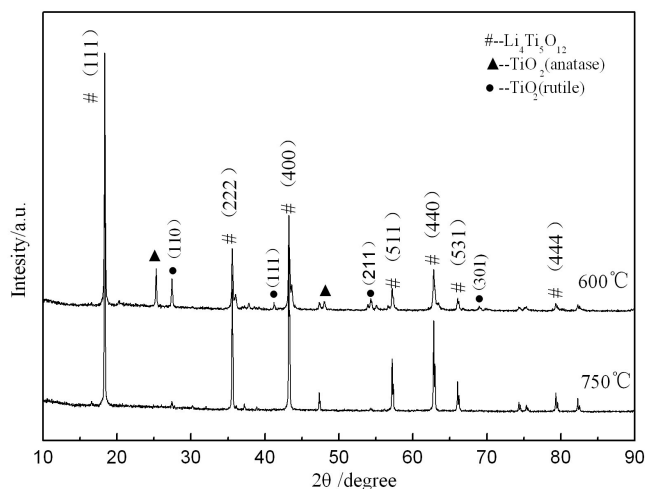


Figure 5. XRD patterns of the as-prepared samples with 8% Li excess calcined at 600 °C and 750 °C for 12h. The main diffraction peaks of  $\text{Li}_4\text{Ti}_5\text{O}_{12}$ , rutile phase  $\text{TiO}_2$  and anatase phase  $\text{TiO}_2$  are marked in the diagram.

precursor, which comes from the hydrolysis of  $\text{Ti}(\text{OC}_2\text{H}_5)_4$ , and another peak centered at 360 °C is attributable to the decomposition of  $\text{LiAc}$ . Above 500 °C, no obvious weight loss is observed in the TGA curve. But the broad endothermic peak observed in the DSC curve indicates the reaction between  $\text{Li}_2\text{O}$  and  $\text{TiO}_2$  continue to occur higher than 500 °C. In order to investigate the effect of Li excess on the crystal structure, the morphology and the electrochemical performance of the  $\text{Li}_4\text{Ti}_5\text{O}_{12}$  anode powders, the following calcination temperature for the dry precursor powders is firstly carried out at 800 °C, assuring the complete reaction.

The XRD patterns and SEM images of the samples calcined at 800 °C for 12h with no Li excess and 8% Li excess are presented in Fig.2 and Fig.3. It can be seen that the primary product for the sample with no Li excess is a mixture of spinel-type  $\text{Li}_4\text{Ti}_5\text{O}_{12}$  phase

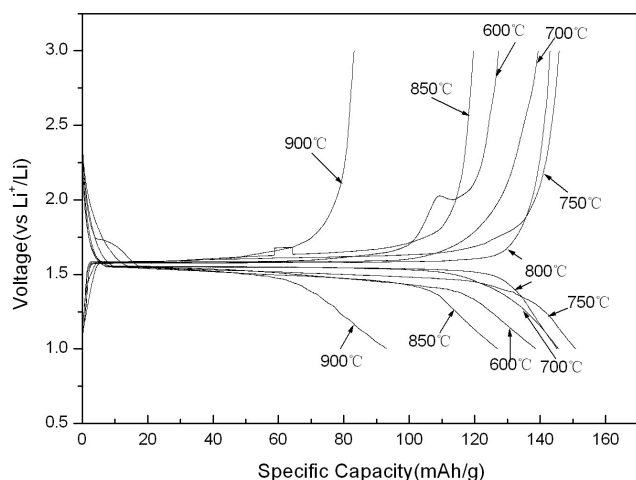


Figure 6. The initial charge-discharge profiles for the as-prepared oxides after the calcination at between 600 °C and 900 °C for 12h at 0.1C rate.

with Ti deficit and rutile-type  $\text{TiO}_2$ . But when 8% excess of Li is considered, very minor amount of rutile  $\text{TiO}_2$  was detected. The mean size of the powders with no Li excess measured from the SEM image is much larger than that of the sample with 8% Li excess due to the fairly existing  $\text{TiO}_2$  phase. The initial charge-discharge test shown in Fig.4 presents that the electrode material with 8% Li excess have the best performance, comparing with the other samples with 0%, 2%, 5% and 10% Li excess. So 8% Li excess is considered hereafter.

Fig.5 shows the XRD patterns of the as-prepared samples with 8% Li excess calcined at 600 °C and 750 °C for 12h. After the calcination at 600°C, the product mainly comprises  $\text{Li}_4\text{Ti}_5\text{O}_{12}$  phase, anatase-type  $\text{TiO}_2$  and rutile-type  $\text{TiO}_2$  based on the XRD results. With the increase of calcination temperature, the peak intensity of the spinel  $\text{Li}_4\text{Ti}_5\text{O}_{12}$  increases greatly, indicating that much more  $\text{Li}_4\text{Ti}_5\text{O}_{12}$  is formed as well as the improved crystallinity of the material with temperature. Meanwhile, no obvious diffraction peaks of rutile  $\text{TiO}_2$  and anatase  $\text{TiO}_2$  are detected after the calcination at 750 °C. But with increasing temperature to 800 °C, the diffraction peaks corresponding to rutile-type  $\text{TiO}_2$  phase emerge again, as shown in Fig.2. This may be attributed to the much more loss of Li by evaporation at temperature higher than 750 °C, which is corresponding to the weight loss in the TGA curve as shown in Fig.1. Therefore, it suggests that the precursor powder from the hydrolysis precipitation can be transformed into spinel  $\text{Li}_4\text{Ti}_5\text{O}_{12}$  after calcination at 750 °C, which greatly increases the precise stoichiometry of the oxide. The sample calcined at 750 °C has a much smaller particle size and a more homogenous distribution than that of the sample calcined at 800 °C as shown in Fig.3.

To clarify the effect of impurity on the electrochemical performance of the  $\text{Li}_4\text{Ti}_5\text{O}_{12}$ , some electrochemical tests were carried out. Fig.6 shows the charge-discharge curves of the as-prepared oxides after the calcination between 600 °C and 900 °C at 0.1 C rate over the potential range of 1.0-3.0 V (versus  $\text{Li}^+/\text{Li}$ ). It can be seen that the oxides calcined between 700 °C and 850 °C exhibit extremely flat discharge/charge plateaus at the voltage about 1.5–1.6V (versus

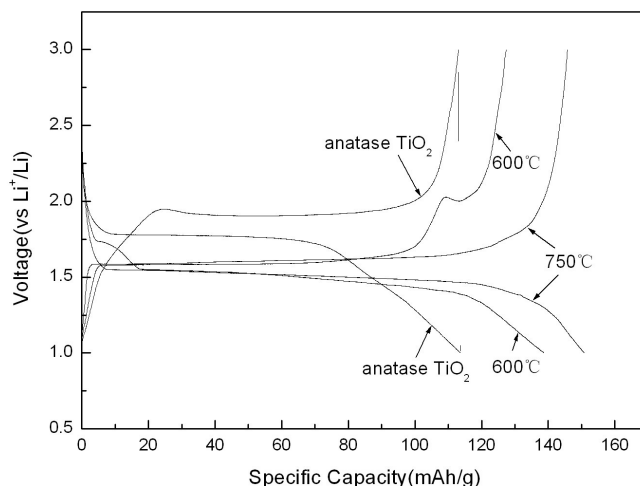


Figure 7. A comparison of discharge and charge curves of pure  $\text{Li}_4\text{Ti}_5\text{O}_{12}$ , anatase  $\text{TiO}_2$  and the as-prepared oxides after the calcination at 600 °C at 0.1 C rate.

$\text{Li}^+/\text{Li}$ ), which is an intrinsic electrochemical property of spinel  $\text{Li}_4\text{Ti}_5\text{O}_{12}$ . Moreover, the small potential difference between charge and discharge plateau is only 60 mV, indicating that the polarization of all the samples is very low. However, the charge plateau of the sample after the calcination at 900 °C departs from the standard potential gradually. The main reason is perhaps due to the high lithium deficiency in  $\text{Li}_4\text{Ti}_5\text{O}_{12}$  from the evident lithium evaporation at high temperature, which causes the high polarization of the electrode. The sample calcined at 750 °C exhibits the best electrochemical performance with a discharge specific capacity of  $152 \text{ mAh}\cdot\text{g}^{-1}$  and 97% coulombic efficiency, while the sample calcined at 900 °C exhibits a specific capacity of only  $92.5 \text{ mAh}\cdot\text{g}^{-1}$  in the first cycle.

Different from the anodes prepared from the calcination higher than 700 °C, which show only one discharge/charge voltage platform at  $\sim 1.5 \text{ V}/\sim 1.6 \text{ V}$ , the 600 °C calcined one shows two discharge/charge platforms, one around 1.7 V/1.9 V and the other at  $\sim 1.5 \text{ V}/1.6 \text{ V}$ . As observed in Fig.5, the 600 °C calcined sample is characterized by the presence of noticeable amount of anatase-type  $\text{TiO}_2$  impurity. And some literatures also testified that the discharge/charge platform at  $\sim 1.7 \text{ V}/1.9 \text{ V}$  is an intrinsic electrochemical property of anatase  $\text{TiO}_2$  [33-35]. We also synthesized anatase  $\text{TiO}_2$  through the hydrolysis precipitation without adding the LiAc and tested the pure anatase-type as the anode at the discharge/charge rate of 0.1 C. As shown in Fig.7, broad discharge and charge platforms are observed at the voltages of 1.8 V and 1.9 V, respectively. Such results strongly support that the second discharge/charge platforms for the 600 °C calcined sample are originated from the lithium intercalation and de-intercalation into the impurity phase of anatase-type  $\text{TiO}_2$  in the anode.

The cycling stability of the 750 °C calcined sample with 8% Li excess, which has the highest initial discharge capacity, is shown in Fig.8. High cycling stability was observed. At 0.1 C rate, the decay in discharge capacity after the 7 cycles was only 2.6%. It suggests the high reversibility and stability of the Li-intercalation and de-

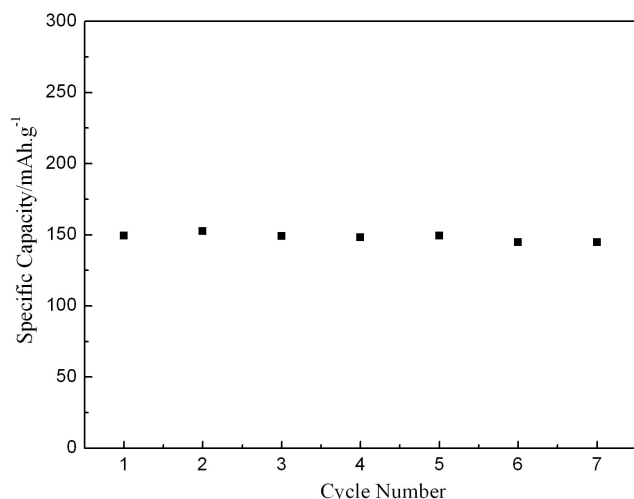


Figure 8. Discharge capacities versus cycle number for the as-prepared sample with 8% Li excess calcined at 750 °C for 12 h at 0.1 C rate.

intercalation through the as-prepared  $\text{Li}_4\text{Ti}_5\text{O}_{12}$ .

The spinel  $\text{Li}_4\text{Ti}_5\text{O}_{12}$  with smallest possible particle size and highest possible phase purity exhibits the best electrochemistry performance. So the lowest possible temperature is needed to synthesize phase pure and well-crystallized  $\text{Li}_4\text{Ti}_5\text{O}_{12}$  nanoparticles via a solid state route, which is the most attractive process. Different from the conventional solid-state reaction, the hydrolysis precipitation as the precursor is obtained firstly in this study. The precise control and uniform mixing of the reactants are realized, which is very important to the preparation of pure  $\text{Li}_4\text{Ti}_5\text{O}_{12}$ . Meanwhile, the newly formed reactant mixture is highly likely to be interconnected with each other and the reactivity of them is elevated through the hydrolysis precipitation reaction, which will decrease the following calcination temperature finally.

#### 4. CONCLUSION

We have synthesized spinel  $\text{Li}_4\text{Ti}_5\text{O}_{12}$  materials as the negative electrode for Li-ion batteries using a hydrolysis precipitation-assisted solid state method. The influence of hydrolysis precipitation is positive to the preparation of  $\text{Li}_4\text{Ti}_5\text{O}_{12}$  at the lowest temperature. A pure  $\text{Li}_4\text{Ti}_5\text{O}_{12}$  phase not containing an impurity phase is obtained based on the XRD measurements, when the precipitation precursor mixture with 8% excess lithium is calcined at 750 °C for 12h. The as-obtained  $\text{Li}_4\text{Ti}_5\text{O}_{12}$  powder is in a narrow size distribution. Accordingly, it shows the higher capacity of  $\sim 152 \text{ mAh.g}^{-1}$  at 0.1 C rate, comparing with the  $\text{Li}_4\text{Ti}_5\text{O}_{12}$  products containing impurity phases, such as rutile  $\text{TiO}_2$  and/or anatase  $\text{TiO}_2$ .

#### 5. ACKNOWLEDGEMENTS

This work was financially supported by the Zhejiang Analysis Test Project of China (2009F70010).

#### REFERENCES

- [1] T. Ohzuku, A. Ueda, and N. Yamamoto, *J. Electrochem. Soc.*, 142, 1431(1995).
- [2] K.M. Colbow, J.R. Dahn, and R.R. Haering, *J. Power Sources*, 26, 397 (1989).
- [3] E. Ferg, R.J. Gummov, A. de Kock, and M.M. Thacheray, *J. Electrochem. Soc.*, 141, L147 (1994).
- [4] K. Zaghib, M. Dontigny, A. Guerfi, P. Charest, I. Rodrigues, A. Mauger, and C.M. Julien, *J. Power Sources*, 196, 3949(2011).
- [5] K. Ariyoshi, S. Yamamoto, and T. Ohzuku, *J. Power Sources*, 119–121, 959 (2003).
- [6] D. Peramunage, and K.M. Abraham, *J. Electrochem. Soc.*, 145, 2609 (1998).
- [7] A.D Pasquier, and C.C. Huang, *J. Power Sources*, 186, 508 (2009).
- [8] C.M. Ionica-Bousquet, D. Muñoz-Rojas, W.J. Casteel, R.M. Pearlstein, G. GirishKumar, G.P. Pez, and M.R. Palacín, *J. Power Sources*, 195, 1479 (2010).
- [9] G.G. Amatucci, F. Badway, A. Du Pasquier, and T. Zheng, *J. Electrochem. Soc.*, 148, A930 (2001).
- [10] L. Kavan, J. Procházka, T.M. Spitler, M. Kalbá, M. Zukulová, T. Drezen, and M. Grätzel, *J. Electrochem. Soc.*, 150, A1000 (2003).
- [11] W.J.H. Borghols, M. Wagemaker, U. Lafont, E.M. Kelder, and F.M. Mulder, *J. Am. Chem. Soc.*, 131, 17786 (2009).
- [12] A.S. Arico, P. Bruce, B. Scrosati, J.M. Tarascon, and W. Van Schalkwijk, *Nat. Mater.*, 4, 366 (2005).
- [13] B.J. Hwang, R. Santhanam, and D.G. Liu, *J. Power Sources*, 97–98, 443 (2001).
- [14] K. Kanamura, T. Chiba, and K. Dokko, *J. Eur. Ceram. Soc.*, 26, 577 (2006).
- [15] D. Yoshikawa, Y. Kadoma, J.M Kim, K. Ui, N. Kumagai, N. Kitamura, and Y. Idemoto, *Electrochim. Acta*, 55, 1872 (2010).
- [16] Y.F. Tang, L. Yang, Z. Qiu, and J.S. Huang, *Electrochem. Commun.*, 10, 1513 (2008).
- [17] J. Li, Z. Tang, and Z. Zhang, *Electrochem. Commun.*, 7, 894 (2005).
- [18] C. Lai, Y.Y. Dou, X. Li, and X.P. Gao, *J. Power Sources*, 195, 3676 (2010).
- [19] S. Bach, J.P. Pereira-Ramos, and N. Baffier, *J. Power Sources*, 81–82, 273 (1999).
- [20] Y.H. Rho, K. Kanamura, M. Fujisaki, J. Hamagami, S. Suda, and T. Umegaki, *Solid State Ionics*, 151, 151 (2002).
- [21] C.M. Shen, X.G. Zhang, Y.K. Zhou, and H.L. Li, *Mater. Chem. Phys.*, 78, 437 (2002).
- [22] Y. J. Hao, Q. Y. Lai, Z. H. Xu, and X.Y. Ji, *Solid State Ionics*, 176, 1201 (2005).
- [23] C.H. Jiang, Y. Zhou, I. Honma, T. Kudo, and H.S. Zhou, *J. Power Sources*, 166, 514 (2007).
- [24] M. Venkateswarlu, C.H. Chen, J.S. Do, C.W. Lin, T.C. Chou, and B.J. Hwang, *J. Power Sources*, 146, 204 (2005).
- [25] N.A. Alias, M.Z. Kufian, L.P. Teo, S.R. Majid, and A.K. Arof, *J. Alloys Compd.*, 486, 645 (2009).

- [26]K.M. Colbow, J.R. Dahn, and R.R. Haering, *J. Power Sources*, 26, 397 (1989).
- [27]E. Ferg, R.J. Gummov, A. de Kock, and M.M. Thacheray, *J. Electrochem. Soc.*, 141, L147 (1994).
- [28]Y. Abe, E. Matsui, and M. Senna, *J. Phys. Chem. Solids*, 68, 681 (2007)
- [29]K. Nakahara, R. Nakajima, T. Matsushima, and H. Majima, *J. Power Sources*, 117, 131 (2003).
- [30]K. Zaghbi, M. Simoneau, M. Armand, and M. Gauthier, *J. Power Sources*, 81–82, 300 (1999).
- [31]S.I. Pyun, S.W. Kim, and H.C. Shin, *J. Power Sources*, 81–82, 248 (1999).
- [32]A. Guerfi, P. Charest, K. Kinoshita, M. Perrier, K. Zaghbi, *J. Power Sources* 126, 163 (2004).
- [33]V. Subramanian, A. Karki, K.I. Gnanasekar, F. Posey Eddy, and B. Rambabu, *J. Power Sources*, 159, 186 (2006).
- [34]J.P. Wang, Y.Bai, M.Y. Wu, J. Yin, and W.F. Zhang, *J. Power Sources*, 191, 614 (2009).
- [35]J.Z. Chen, L. Yang, and Y.F. Tang, *J. Power Sources*, 195, 6893 (2010).